

1 **Multiple Displacement Amplification Facilitates SMRT Sequencing of Microscopic**  
2 **Animals and the Genome of the Gastrotrich *Lepidodermella squamata* (Dujardin, 1841)**

3 Nickellaus G. Roberts<sup>1</sup>, [ngroberts@crimson.ua.edu](mailto:ngroberts@crimson.ua.edu)  
4 Michael J. Gilmore<sup>1</sup>, [gilmore.michael1999@gmail.com](mailto:gilmore.michael1999@gmail.com)  
5 Torsten H. Struck<sup>2</sup>, [t.h.struck@nhm.uio.no](mailto:t.h.struck@nhm.uio.no)  
6 \*Kevin M. Kocot<sup>1,3</sup> ,[kmkocot @ua.edu](mailto:kmkocot@ua.edu)

7 <sup>1</sup>Department of Biological Sciences, The University of Alabama, <sup>2</sup>Natural History Museum,  
8 University of Oslo, <sup>3</sup>Alabama Museum of Natural History

9 \*Corresponding author.

10

11

12

13

14

15

16

17

18

19

20 **Abstract:**

21 **Background:**

22 Obtaining adequate DNA for long-read genome sequencing remains a roadblock to producing  
23 contiguous genomes from small-bodied organisms. Multiple displacement amplification (MDA)  
24 leverages Phi29 DNA polymerase to produce micrograms of DNA from picograms of input. Few  
25 genomes have been generated using this approach, due to concerns over biases in amplification  
26 related to GC and repeat content and chimera production. Here, we explored the utility of MDA  
27 for generating template DNA for PacBio HiFi sequencing using *Caenorhabditis elegans*  
28 (Nematoda) and *Lepidodermella squamata* (Gastrotricha).

29 **Results:**

30 HiFi sequencing of libraries prepared from MDA DNA produced highly contiguous and  
31 complete genomes for both *C. elegans* (102 Mbp assembly; 336 contigs; N50 = 868 Kbp; L50 =  
32 39; BUSCO\_nematoda: S:92.2%, D:2.7%) and *L. squamata* (122 Mbp assembly; 157 contigs;  
33 N50 = 3.9 Mb; L50 = 13; BUSCO\_metazoa: S: 78.0%, D: 2.8%). Amplified *C. elegans* reads  
34 mapped to the reference genome with a rate of 99.92% and coverage of 99.75% with just one  
35 read (of 708,811) inferred to be chimeric. Coverage uniformity was nearly identical for reads  
36 from MDA DNA and reads from pooled worm DNA when mapped to the reference genome. The  
37 genome of *Lepidodermella squamata*, the first of its phylum, was leveraged to infer the  
38 phylogenetic position of Gastrotricha, which has long been debated, as the sister taxon of  
39 Platyhelminthes.

40 **Conclusions:**

41 This methodology will help generate contiguous genomes of microscopic taxa whose body size  
42 precludes standard long-read sequencing. *L. squamata* is an emerging model in evolutionary  
43 developmental biology and this genome will facilitate further work on this species.

44

45 **Background:**

46 In recent years, long-read technologies have become the industry standard for *de novo* genome  
47 sequencing. Pacific Biosciences' (PacBio) multiple pass circular consensus sequencing (HiFi)  
48 has stood out as a popular choice for *de novo* genome sequencing due to its high accuracy (base-  
49 level resolution of >99%) and relatively long reads (~10 Kbp) able to cover complex and  
50 repetitive genomic regions (Hon et al. 2020). Using adequate high-molecular-weight (HMW)  
51 DNA with as little damage as possible for sequencing library preparation is crucial to obtain  
52 reads that are both highly accurate and of adequate length (Pollard et al. 2018). Avoiding pooling  
53 multiple individuals serves to increase the assembly quality of genomes by reducing  
54 heterozygosity (Birky 1996; Flot et al. 2013; Huang et al. 2017; Simion et al. 2018). It follows  
55 that *de novo* genome projects are most likely to succeed when a large amount of unfragmented,  
56 HMW DNA with little to no exogenous contamination is available from a single individual.

57 Unfortunately, obtaining such amounts of starting material meeting the above requirements is not  
58 always possible. PacBio's Ultra-Low DNA Input Workflow yields data volumes comparable to  
59 standard input libraries from as little as 5 ng of HMW template. This approach has successfully  
60 been used to produce high-quality genomes from individual small animals such as mosquitos  
61 (Kingan et al. 2019) and springtails (Schneider et al. 2021). However, even the Ultra-Low DNA  
62 Input Workflow is not applicable to very small animals (e.g., < 1 mm total length). For example,

63 a single hermaphrodite specimen of *Caenorhabditis elegans* contains 959 somatic nuclei (Cohen-  
64 Fix and Askjaer 2017) and has a genome size of roughly 100 Mbp (*C. elegans* Sequencing  
65 Consortium 1998) meaning that a single specimen may contain as little as 200 picograms of  
66 DNA with comparable DNA content in other small-bodied phyla, also ranging in the hundreds of  
67 picograms of maximal yield. Thus, obtaining sufficient starting material meeting even the greatly  
68 reduced input requirements for the PacBio Ultra-Low DNA Input Workflow is not possible for  
69 many organisms. Further, if researchers want to avoid pooling multiple individuals or if the  
70 organism of interest is both small and rare, reduced input strategies are not an option thus far.

71 It is of little debate that for most applications leveraging genomes, assemblies that are both  
72 contiguous and well-annotated are ideal (reviewed by Laumer 2018). However, due to the  
73 challenges associated with sequencing genomes of small-bodied animals, metazoan genome  
74 sequencing efforts have been biased towards large-bodied organisms. Of the roughly 30  
75 metazoan phyla, nearly all those that are still lacking high quality genome assemblies – or any  
76 genomic data at all in some cases – are small-bodied (Worsaae et al. 2023). For example, within  
77 Lophotrochozoa (=Spiralia) all phyla that are lacking in genomic data are mostly or exclusively  
78 small-bodied (Figure 1, Figure S1). With an average body size of <1 mm, these organisms are  
79 underrepresented in genomic and phylogenomic studies (Kocot et al. 2017; Laumer et al. 2019).

80 Whole genome amplification (WGA) methodologies are of great use to the fields of diagnostic  
81 medicine and single cell research (Evrony et al. 2015; Fu et al. 2015; Li et al. 2018; Zhou et al.  
82 2020), but their utility in amplifying DNA for sequencing very small-bodied organisms in the  
83 age of long-read sequencing technologies has received little attention (but see Lee et al. 2023).  
84 WGA is a popular strategy for generating large amounts of DNA from limiting sample material  
85 through techniques such as multiple displacement amplification (MDA) (Dean et al. 2001),

86 degenerate-oligonucleotide-primed-PCR (DOP-PCR) (Telenius et al. 1992), DOP-PCR (Telenius  
87 et al. 1992), PEP-PCR (Moghaddaszadeh-Ahrabi et al. 2012), LM-PCR (Carey MF et al. 2009),  
88 T-PCR (Tarr AW et al. 2005), and multiple annealing and looping based amplification cycles  
89 (MALBAC) (Chapman et al. 2015). However the use of WGA for long-read sequencing library  
90 preparation has largely been limited to the detection of structural variants, large deletions and  
91 inversions, and amplicon sequencing from degraded material (Evrony et al. 2015; Zhou et al.  
92 2020).

93 WGA methodologies typically make use of PCR, isothermal amplification, or both (reviewed by  
94 Wang et al. 2022). PCR based protocols make use of specific primers, degenerate oligos, and/or  
95 repetitive genomic regions for priming. These strictly PCR-based amplification strategies are  
96 exponential and thus uneven or non-specific amplification may occur due to variation in template  
97 GC content and amplicon length. PCR-based methodologies have been used in medical and  
98 diagnostic approaches for their ability to analyze copy number variation and identify small  
99 structural variants or small stretches of SNP variation, but their utility for long-read sequencing  
100 is limited due to typical product fragment sizes only being within 100-1000 bp. Long-range PCR  
101 based approaches have been demonstrated to be successful for *de novo* genome sequencing of  
102 specimens in which material is limited (Laumer 2023; Stevens et al. 2023). Picogram input  
103 multimodal sequencing (PiMmS) makes use of oligo-dT beads to separate cDNA and genomic  
104 DNA from the same individual, providing transcript evidence from the same individual for  
105 downstream gene annotation. PiMmS amplification technique involves DNA purification using a  
106 salting out procedure to provide HMW ethanol-precipitated DNA. As PiMmS makes use of  
107 PCR, a qPCR step is required to estimate cycle number to reduce artifacts produced during PCR  
108 amplification.

109 Isothermal amplification in the case of MDA uses Phi29 DNA polymerase to amplify long  
110 fragments of linear or circular DNA (Dean et al. 2001; Dean et al. 2002; Lasken 2007).  
111 Amplification using Phi29 polymerase is highly accurate due to high strand-displacement  
112 activity, extremely high processivity, and strong proofreading activity (Garmendia et al. 1992).  
113 MDA, as opposed to PCR-based WGA approaches, has the benefit of producing highly accurate  
114 fragments with an average fragment length greater than 10 Kbp (up to 100 Kbp). Like other  
115 WGA approaches, MDA can produce tens of micrograms of DNA from picograms of starting  
116 material. MDA typically makes use of short, random exonuclease-resistant primers to allow the  
117 reaction to proceed isothermally. Like PCR-based methods, MDA is exponential leading to  
118 potential biases in coverage based on GC content (Lasken and Egholm 2003; Borgström et al.  
119 2017). In GC-rich regions, there may be reduction of polymerase processivity leading to  
120 underrepresentation of that region during amplification. However, differential binding affinities  
121 of GC- and AT-rich primers can lead to GC-rich regions being preferentially amplified (Benita et  
122 al. 2003; Sahdev et al. 2007). Further, the denaturation strategy used prior to MDA (alkali,  
123 thermal or otherwise) may affect access and efficacy of DNA binding in GC rich regions. For  
124 example, KOH alkali denaturation has been shown to increase primer access to GC rich template  
125 DNA (Pinard et al. 2006). Such amplification bias with respect to GC richness is a function of  
126 reaction gain, defined as the ratio of DNA product mass over DNA template mass. Compared to  
127 MALBAC and PicoPLEX single cell, increased reaction gain in the case of MDA more  
128 negatively influences amplification coverage, uniformity, and the detection of copy number  
129 variants (CNVs). However, unlike both MALBAC and PicoPLEX, MDA reactions with high  
130 gain do not have a meaningful increase in the rate of single nucleotide errors (de Bourcy et al.  
131 2014). Fortunately, lowering amplification time reduces reaction gain, thus reducing the over-

132 amplification of certain genomic regions (Dean et al. 2001), making MDA protocols with more  
133 modest amplification time preferable to generate template for *de novo* sequencing. Lowering  
134 reaction gain also can also reduce chimera formation. During MDA, chimeric DNA fragments  
135 can form when 3' termini are displaced and anneal to nearby displaced 5' strands, forming  
136 chimeric DNA fragments that are eventually made into double stranded DNA after random  
137 hexamer annealing and extension (Lasken and Stockwell 2007). Previous studies have suggested  
138 a rate of up to 1 chimera/10 Kbp for MDA, which is problematic for the recovery of specific  
139 genomic regions, the analysis of copy number variation and *de novo* assembly, although these  
140 problems can be reduced with adequate coverage (Rodrigue et al. 2009). Proper preservation of  
141 samples and HMW DNA extraction (resulting in fewer 3' termini) can reduce chimera formation  
142 (Nelson 2014), especially when combined with lower reaction gain. Moreover, as MDA can be  
143 applied directly to lysed cells (Hosono et al. 2003), shearing of DNA during extraction can be  
144 avoided altogether when aliquots of cell cultures or entire microscopic organisms are lysed  
145 followed by immediate amplification in the same tube. Taken together, MDA's isothermal  
146 nature, high accuracy, production of fragments longer than typical PacBio HiFi reads, and ability  
147 to amplify DNA directly from freshly lysed cells makes it an attractive choice for template  
148 preparation for HiFi sequencing. Under low reaction gain and in low volumes, sequencing of  
149 MDA DNA can achieve high data uniformity and coverage (Li et al. 2018). Thus, MDA was  
150 chosen for this study.

151 Here, we investigated the utility of MDA for generating adequate template DNA for PacBio  
152 long-read sequencing from very small animals (<1 mm). We demonstrate the utility of this  
153 approach using the model organism *Caenorhabditis elegans*, which was selected because a high-  
154 quality reference genome and HiFi reads generated from unamplified DNA extracted from a pool

155 of worms are already available for comparison. We additionally chose the gastrotrich  
156 *Lepidodermella squamata* (Dujardin 1841) as a test of MDA's ability to assist in the *de novo*  
157 long-read sequencing of a non-model organism. Gastrotricha (Metschnikoff, 1865), colloquially  
158 referred to as "hairy bellied worms" is a phylum of approximately 749 species of microscopic  
159 benthic invertebrates found in aquatic habitats worldwide (Margulis and Schwartz 1998). Of  
160 these, 346 are found in freshwater habitats, with the rest inhabiting marine and brackish water.  
161 Gastrotricha is composed of two orders, Chaetonotida (Remane, 1925), which include both fresh  
162 and marine species, and Macrodasyida (Remane, 1925), which is an almost exclusively marine  
163 clade. Living mostly in sandy, benthic habitats, key taxonomic characters of Gastrotricha include  
164 the variable presence of scales, spines, or hooks on the body wall and the presence of adhesive  
165 tubes for attaching to substrate. Gastrotrichs typically range from 70  $\mu\text{m}$  to 1 mm in size,  
166 although they may reach up to 3 mm in the case of the genus *Megadasys* (Schmidt, 1974,  
167 Fontaneto et al. 2015). Additionally, gastrotrichs are flattened along their dorsal-ventral axis  
168 reducing their volume even further in comparison to similar sized animals with a round body  
169 plan. The  $\sim$ 250  $\mu\text{m}$  freshwater gastrotrich *L. squamata* has proven to be a useful species for the  
170 study of Gastrotricha due to its ease of culture in a freshwater solution containing wheat grains  
171 inoculated with fungi, protozoa, and bacteria (Bennett 1979). Gastrotricha is of great interest to  
172 evolutionary biologists as its phylogenetic position has long been debated (Edgecombe et al.  
173 2011; Struck et al. 2014; Laumer et al. 2015; Kocot 2016; Bleidorn 2019). Availability of a high-  
174 quality reference genome for *L. squamata* would also to the field of evolutionary developmental  
175 biology as *L. squamata* is an emerging model species (Hejnol 2015).

176

177 **Results:**

178 Genome Assembly

179 Sequencing of a HiFi library generated from MDA DNA for *C. elegans* resulted in 708,811 HiFi  
180 reads (96x coverage of the 102.5 Mbp genome) with an average HiFi read length of 13,885 bp.  
181 The *de novo* *C. elegans* assembly was 102 Mbp contained in 336 contigs with an N50 of 868  
182 Kbp and an L50 of 39. The *de novo* assembly was screened for contamination with Blobtools  
183 (Laetsch and Blaxter 2017), however all contigs had hits only to Metazoa (336) and thus none  
184 were removed. The *de novo* assembly had a BUSCO metazoa\_odb10 score of 69.9% (Single  
185 copy BUSCOs [S]:67.5%, Duplicate BUSCOs [D]:2.4%) and a BUSCO nematoda\_odb10 score  
186 of 94.9% (S:92.2%, D:2.7%) compared to 51.3% (S:50.7%, D:0.6%) and 98.5% (S:98.0%,  
187 D:0.5%), respectively, for the reference. The reference-guided *C. elegans* assembly was 102.5  
188 Mbp contained in 281 contigs with an N50 of 16.9 Mbp and an L50 of 3 (Table 1).

189 Sequencing of *L. squamata* resulted in 917,258 HiFi reads with an average HiFi read length of  
190 13,358 bp. The *L. squamata* assembly was 147 Mbp contained in 527 contigs with an N50 of 2.9  
191 Mbp and an L50 of 13. After filtering with Blobtools, 370 contigs were removed based on best  
192 hits to non-metazoans. The resulting assembly was 122 Mbp contained in 157 contigs with an  
193 N50 of 3.9 Mbp and an L50 of 13. BUSCO analysis of the decontaminated assembly using the  
194 metazoa\_odb10 dataset was 80.8% (Single copy BUSCOs [S]: 78.0%, Duplicate BUSCOs [D]:  
195 2.8%; Table 1).

196 **Table 1.** Assembly Statistics for *C. elegans* and *L. squamata*

<i>Organism:</i>	<i>HiFi</i>	<i>Genome</i>	<i>Contigs:</i>	<i>N50</i>	<i>L50</i>	<i>BUSCO</i>	<i>BUSCO</i>
	<i>Reads:</i>	<i>Size</i>		<i>(Mb)</i>	:	<i>metazoa_odb</i>	<i>nematoda_odb</i>
		<i>(Mb):</i>			:	<i>10</i>	<i>10</i>
<i>Lepidodermell</i>	917258	122	157	3.9	13	80.8%	
<i>a squamata</i>						(S: 78.0%,	N/A
<i>[MDA]</i>						D: 2.8%)	
<i>Caenorhabditi</i>	708811	102	336	0.87	39	69.9%	94.9%
<i>s elegans</i>						(S: 67.5%,	(S: 92.2%, D:
<i>[MDA]</i>						D: 2.4%)	2.7%)
<i>Caenorhabditi</i>	N/A	102.5	281	16.9	3	51.3%	98.5%
<i>s elegans</i>						(S: 50.7%,	(S: 98.0%, D:
<i>[Reference</i>						D: 0.6%)	0.5%)
<i>Guided MDA]</i>							

197

198 Coverage and Amplification Bias Estimation

199 Due to MDA's potential for amplification bias with respect to GC and repeat content (Lasken  
200 and Egholm 2003; Borgström et al. 2017), we investigated the relationship between GC and  
201 repeat content and read coverage using the model organism *C. elegans* and its reference genome.  
202 To understand the level as to which MDA may have resulted in over amplification of genomic  
203 regions with respect to GC content, we compared mean coverage in 100 Kbp blocks of reads  
204 from our dataset based on MDA and reads from unamplified DNA extracted from a pool of

205 worms (NCBI SRR22507561) mapped to the reference genome (GCA\_000002985.3) (Figure 2,  
206 Figure S2). Due to the potential for repetitive regions to have GC content far outside the mean,  
207 we also investigated coverage with respect to repeat percentage. The reference *C. elegans* Bristol  
208 N2 genome has a GC content of 35% (GCA\_000002985.3) and, according to RepeatModeler, it  
209 has a repeat content of 18.40%. Mean coverage was normalized for each dataset by subtracting  
210 the minimum mean coverage from each datapoint (representing a 100 Kbp region) divided by the  
211 range of the dataset  $[(x - \min(x))/\text{range}(x)]$ ,  $x$  = coverage of 100 Kbp region]. Resulting  
212 normalized mean coverage, repeat content, and GC content in 100 Kbp blocks across all six  
213 chromosomes were plotted to visualize potential over-amplification of genomic regions during  
214 MDA (Figure 3, Figure 4A-B, Figure S3, Figure S4). This revealed that while some genomic  
215 regions showed over-amplification, amplification across the chromosome was consistent enough  
216 to provide adequate coverage. Plotting normalized coverage against GC content revealed  
217 virtually no difference between data generated from amplified and unamplified DNA (Figure 2)  
218 and the distribution was very uniform with respect to GC content with a few outliers.  
219 Surprisingly, the reads generated from unamplified DNA were more skewed towards higher  
220 coverage for GC values above the mean.

221 Lorenz curves, defined here as a plot of the cumulative share of reads against cumulative share  
222 of genomic positions covered by those reads, ordered from highest to lowest (Zong et al. 2012;  
223 de Bourcy et al. 2014) were calculated (Figure 4, D). The Gini index is calculated as the area  
224 between the calculated Lorenz curve, from the dataset, and a straight Lorenz curve, representing  
225 perfect uniform coverage. In our case, a Gini index of zero would indicate perfect uniform  
226 coverage and a Gini index of 1 would indicate maximally non-uniform coverage. The Gini index  
227 values for the amplified and unamplified datasets were nearly identical, 0.14 and 0.16,

228 respectively, revealing that the uniformity of coverage between the unamplified and amplified *C.*  
229 *elegans* read sets is similar. This suggests little to no effect of MDA amplification bias on  
230 coverage uniformity in the case of *C. elegans*. Coverage statistics, including mean coverage  
231 above and below mean GC content are summarized in Table 2.

232 **Table 2.** *Coverage Statistics and Gini index values for C. elegans and L. squamata unmapped*  
233 *reads.*

<i>Mapped Reads:</i>	<i>Mean Coverage</i>	<i>Mean Coverage of 100 Kbp regions</i>	<i>Mean Coverage of 100 Kbp regions below mean</i>	<i>Gini Index</i>
<i>Across all 100 Kbp Blocks:</i>	<i>above mean GC content.</i>			:
<i>C. elegans [MDA]</i>	98 [SD +/- 62]	102 [SD +/- 77]	92 [SD +/- 19]	0.14
<i>C. elegans [Unamplified]</i>	136 [SD +/- 69]	136 [SD +/- 77]	136 [SD +/- 19]	0.16
<i>L. squamata [MDA]</i>	117 [SD +/- 102]	142 [SD +/- 135]	118 [SD +/- 42]	0.29

234

235 Without a reference genome, no mapping comparisons could be made for *L. squamata*, however  
236 reads were mapped to the primary assembly after removal of contamination with Blobtools to  
237 assess coverage with respect to GC content and repeat content. The resulting genome assembly  
238 of *L. squamata* has a GC content of 43% and a repeat content of 21.98%. A Lorenz curve was

239 plotted and the Gini index was calculated as described above. This resulted in a Gini index of  
240 0.29 indicating less uniform coverage than both *C. elegans* reads based on MDA DNA and reads  
241 based on unamplified DNA (Figure 4D). *L. squamata* was comparatively not as uniform with  
242 respect to GC and repeat content as observed for *C. elegans* showing higher coverage in  
243 repetitive regions (Figure 4C), which also happen to have higher than mean GC richness. While  
244 few 100 Kbp blocks with average and lower GC content have higher fold coverage (Figure 5,  
245 Figure S5), a very substantial part of the coverage at GC content values above 45% exhibits very  
246 high coverage at a repeat content higher than 50% (Figure 6, Figure S6). This indicates possible  
247 preferential amplification of repetitive regions with high GC content. Coverage statistics,  
248 including mean coverage above and below mean GC content are summarized in Table 2.

249 Annotation of *L. squamata* genome

250 BRAKER predicted 28,377 gene models with a BUSCO score of 79.80% (76.4% single-copy  
251 and 3.2% duplicated). The final assembly was estimated to be 21.98% repetitive. Of the 122  
252 Mbp assembly, ~16 Mbp (13.74%) was composed of unclassified repeats, while the remaining  
253 ~26 Mbp (8.24%) was composed of simple repeats.

254 Phylogenetic Analysis

255 To infer the phylogenetic position of Gastrotricha within Lophotrochozoa, we identified  
256 orthologs in the genomes of 23 lophotrochozoans (plus five outgroup taxa) broadly spanning the  
257 diversity of the group. We assembled a supermatrix of 2,779 genes totaling 676,632 amino acids  
258 with 18.68% missing data. Maximum likelihood analysis using the posterior mean site frequency  
259 model (PMSF) (Wang et al. 2018) fitting the C60 profile mixture model resulted in a tree with  
260 full bootstrap support for all nodes (Figure 7). Gastrotricha was recovered as the sister taxon of

261 Platyhelminthes with maximal support, recapitulating the proposed sister-group relationship  
262 recovered previously (Struck et al. 2014) and dubbed Rousphozoa. Rotifera, the only  
263 representative of Gnathifera in this study, was recovered as the sister group to all other  
264 Lophotrochozoa with Rousphozoa as the next branching lineage and the sister taxon of all  
265 remaining taxa (Trochozoa) consistent with Struck et al. (2014). Within Trochozoa, we recover  
266 Mollusca as the sister taxon of a clade comprising, Annelida, Nemertea and the Lophophorate  
267 phyla (Brachiopoda, Bryozoa, and Phoronida), consistent with several previous studies (Struck et  
268 al. 2014; Kocot et al. 2017; Laumer et al. 2019). Due to the tree being based exclusively on  
269 genomes, several lineages of the superphylum, specifically most gnathiferan phyla  
270 (Chaetognatha, Gnathostomulida and Micrognathozoa), Cycliophora, and Entoprocta could not  
271 be included in this analysis.

272

### 273 **Discussion:**

274 Here, we investigated the utility of MDA for generating adequate template DNA from small-  
275 bodied organisms for PacBio HiFi sequencing. Although coverage uniformity with respect to GC  
276 and repeat content are known biases of MDA, our results show that MDA of DNA obtained  
277 directly from lysed cells can be used to generate template for HiFi sequencing with limited  
278 coverage bias and artifacts.

279 Given existing high-quality genomic resources, *C. elegans* was chosen to explore the uniformity  
280 of coverage with respect to GC and repeat content by comparing our HiFi data generated from  
281 MDA DNA to HiFi data generated from unamplified DNA extracted from a pool of worms.  
282 Compared to HiFi reads generated unamplified DNA (Gini Index of 0.16), reads generated from

283 MDA DNA (Gini Index of 0.14) performed similarly in terms of coverage uniformity,  
284 demonstrating that starting with samples as small as one-half *C. elegans* does not result in  
285 sequence data with significant amplification bias. While our *de novo* *C. elegans* assembly is not  
286 chromosome-level, it is rather contiguous and performed well in terms of BUSCO completeness  
287 (Table 1). When compared to PacBio Ultra-Low Input assemblies from single organisms, such as  
288 springtails (Schneider et al. 2021), our *C. elegans* assembly exhibits comparable completeness,  
289 albeit with lower contiguity. While our assembly performed well in terms of completeness  
290 (BUSCO Nematoda score of 94.9%), N50 was notably lower (868 Kbp) and the assembly  
291 consisted of a higher number of contigs (336) when compared to both springtail assemblies (N50  
292 = 5.6 Mbp, 142 contigs, 211 Mbp size and N50 = 8.7 Mbp 165 Mbp size, 79 contigs for *Desoria*  
293 *tigrina* and *Sminthurides aquaticus* respectfully). This suggests that the PacBio Ultra-Low Input  
294 Workflow is likely a better choice than our MDA-based strategy for animals that can provide  
295 adequate HMW template DNA (>5 ng), but that would not be possible in the case of *C. elegans*  
296 and many (if not most) meiofaunal animals where a whole animal contains roughly an order of  
297 magnitude less DNA than required.

298 We were also concerned about the potential for formation of chimeras. However, investigation of  
299 inverted sequences and tandem regions with Alvis identified only one suspected chimeric contig  
300 in our *C. elegans* assembly and none in our *L. squamata* assembly, supporting previous  
301 hypotheses about chimera formation being highly correlated with high reaction gain (Lasken and  
302 Stockwell 2007; de Bourcy et al. 2014). Also, because we lysed cells and immediately proceeded  
303 with MDA in the same tube without a DNA extraction procedure, our template DNA underwent  
304 little handling that could cause breakage. This would result in fewer free 3' ends of strands that  
305 could anneal to another strand and act as a primer to initiate chimera formation. As chimeric

306 reads may be more problematic in data obtained from more fragmented template DNA, paired-  
307 end Illumina data generated from half of the specimen lysate before MDA could be used in  
308 future studies to aid in the detection of chimeras (see Lee et al. 2023). Examining the mapping of  
309 paired-end short reads to post-amplification HiFi reads could be used to reveal chimeric reads as  
310 one of the reads in a pair would be expected to map on one side of the chimeric junction while its  
311 mate would be expected to map elsewhere.

312 Our results demonstrate that this approach can be successfully used on small-bodied organisms  
313 without a reference genome to produce assemblies that are both rather contiguous and complete.  
314 The *L. squamata* assembly was rather contiguous with an assembly consisting of 157 contigs and  
315 an N50 of 3.9 Mbp approaching the level of contiguity produced using the PacBio Ultra Low  
316 Input Workflow (Schneider et al. 2021). The inferred BUSCO completeness score of 80.8% for  
317 *L. squamata* based on the metazoa\_odb10 set suggests that this genome is lacking nearly 20% of  
318 the nuclear protein-coding genes thought to be single-copy in all metazoans. However, *L.*  
319 *squamata* is a long-branched taxon in our phylogenomic analysis and Gastrotricha as a phylum  
320 has been shown to be long branched in previous phylogenomic studies (Struck et al. 2014; Kocot  
321 et al. 2017; Laumer et al. 2019; Marlétaz et al. 2019). Moreover, there are no gastrotrichs or  
322 early-branching flatworms in the metazoa\_odb10 reference dataset (Manni et al. 2021). Like the  
323 reference genome of *C. elegans* (BUSCO metazoa\_odb10 score of 51.3%), *L. squamata* may  
324 have performed poorly in this BUSCO analysis due to sequence divergence rather than absence  
325 of these genes, although loss of BUSCOs in compact invertebrate genomes has been reported  
326 previously (Cunha et al. 2023). Regardless, the score recovered here represents a relatively high  
327 level of completeness when compared to other sequenced members of the lophotrochozoan  
328 superphylum (Figure S1). Annotation of the genome resulted in 28,377 genes, which BUSCO

329 found to be 79.8% complete, which is comparable to the BUSCO score for the genome  
330 assembly, suggesting that the predicted gene model set is of high quality. Taken together, these  
331 results demonstrate that MDA combined with highly accurate HiFi sequencing can result in  
332 genome assemblies of similar quality to those of other non-model invertebrates (Rayko et al.  
333 2020).

334 Despite the high contiguity of the *L. squamata* assembly, more bias with respect to repeat  
335 content and GC richness was observed in these data than in those from *C. elegans*. When  
336 compared to the *C. elegans* reference genome (18.40% repeats, 35% GC content), *L. squamata*  
337 (21.98% repeats, 43% GC content) has a higher repeat content. As a result of increased repeat  
338 percentage and higher overall GC content, we observed increased coverage in regions with >45%  
339 GC content, particularly in 100 Kbp blocks containing more than 50% repeats and in relatively  
340 short contigs. Amplification bias in GC-rich regions is a known artifact of MDA (Dean et al.  
341 2002; de Bourcy et al. 2014), and our results provide supporting evidence for this. However,  
342 provided ample coverage, we were still able to capture enough breadth of the genome to produce  
343 a relatively complete and contiguous assembly.

344 MDA has been explored in the context of Oxford Nanopore (ONT) sequencing to produce  
345 relatively contiguous genomes from single nematodes (Lee et al. 2023). For *C. elegans*, the  
346 authors generated an assembly consisting of 499 contigs with an N50 of 656.2 Kbp and a  
347 BUSCO completeness score of 97.6%, compared to 336 contigs with an N50 of 868.1 Kbp and a  
348 BUSCO score of 92.2% in the present study. However, applying this approach to 13 other non-  
349 model nematodes, they recovered genome assemblies ranging from 136.6 Mbp to 738.8 Mbp in  
350 1,557 to 32,219 contigs with N50 values of 26.3 Kbp to 441.0 Kbp. Drops in coverage were  
351 observed around highly repetitive regions but coverage with respect to GC content was not

352 examined in detail. Notably, T7 endonuclease digestion was needed in the case of ONT  
353 sequencing, as MDA's secondary branching products can clog sequencing pores, reducing yield.  
354 Due to the nature of library preparation following shearing and size selection, endonuclease  
355 digestion is not needed for HiFi sequencing, a benefit of the approach presented here.

356 Given the successful application of this method to the organisms studied here, an important  
357 direction for future work would be to apply this strategy to other small-bodied phyla that are  
358 currently lacking published genomes (Chaetognatha, Gnathostomulida, Micrognathozoa,  
359 Entoprocta and Cycliophora). Increased genomic sampling of small-bodied phyla will lead to an  
360 elevated understanding about the evolution of small-bodied organisms and will assist in  
361 uncovering potential signatures and commonalities underlying the genomic architecture of small-  
362 bodied animals. The genomic consequences of miniaturization are poorly understood given the  
363 dearth of genomes from microscopic animals. Work to date has revealed that while some small-  
364 bodied lineages exhibit drastic simplification of genome architecture and reduction in content  
365 with respect to their large-bodied relatives (Seo et al. 2001; Mikhailov et al. 2016), have taken a  
366 more conservative route in regards to genome compaction (Martín-Durán et al. 2021; reviewed  
367 by Worsaae et al. 2023). Increased genomic sampling broadly spanning the metazoan tree stands  
368 to provide insight into genomic signatures of miniaturization. While our results demonstrate the  
369 utility of an MDA-based genome sequencing strategy for small-bodied animals with small  
370 genomes (i.e., 102 Mbp and 122 Mbp), the efficacy of this approach for organisms that are  
371 small-bodied, but with larger genomes still needs rigorous examination.

372 Combination of this approach with other low input sequencing techniques, such as PiMmS  
373 (Laumer, 2022), may be a valuable strategy as these techniques are expected to differ in their  
374 biases with respect to amplification uniformity. In contrast to long-range PCR amplification used

375 in PiMmS and the PacBio Ultra-Low Input Workflow, the isothermal amplification used in  
376 MDA eliminates PCR duplicates at the cost of reduced uniformity across GC rich regions,  
377 particularly those high in repeats (Figure 3, Figure 4A, B). Here, DNA was amplified directly  
378 from lysed cells, bypassing HMW DNA extraction that may result in DNA loss from  
379 exceptionally small specimens and fragmentation, which we view as a beneficial characteristic of  
380 this approach. Careful consideration of the potential amount of DNA in a sample will aid in  
381 decision making regarding amplification directly from lysed cells as performed here versus  
382 HMW DNA extraction. Library diversity and complexity are both important considerations  
383 following any amplification protocol, as low complexity libraries, resulting from degraded or too  
384 little template DNA, can lead to poor quality assemblies. Finally, MDA's yield of large amounts  
385 of DNA from limiting starting material allows multiple sequencing libraries to be produced from  
386 a single round of amplification, making it possible to increase coverage across under-amplified  
387 genomic regions, such as those with lower GC content.

388

389 **Conclusion:**

390 The amount of starting DNA has long been a limiting factor in *de novo* genome projects and,  
391 despite recent advances, many organisms still contain too little DNA for genome sequencing  
392 using available long-read sequencing library preparation protocols. In this study, the efficacy of  
393 whole genome sequencing following multiple displacement amplification with phi29 DNA  
394 polymerase was assessed. We demonstrate that HiFi sequencing data produced from MDA DNA  
395 can successfully lead to a fairly contiguous and complete assembly for both model organisms  
396 such as *C. elegans* (Nematoda) and for non-model organisms such as *L. squamata* (Gastrotricha)

397 with limited coverage bias and an extremely low incidence of chimeras. This methodology could  
398 be further expanded upon or combined with other scaffolding techniques or amplification  
399 strategies to increase the contiguity of genomes from amplified material. This strategy has the  
400 potential to greatly expand the availability of whole genome sequencing data from a wide variety  
401 of DNA-limited sources including but not limited to other microscopic metazoans.

402

## 403 **Materials and Methods**

### 404 Laboratory Methods

405 Live cultures of *C. elegans* (Bristol N2) and *L. squamata* were purchased from Carolina  
406 Biological Supply Co. and kept alive in the laboratory under manufacturer recommended  
407 conditions. Half of a single individual *C. elegans* hermaphrodite (~500 µm) cut with a sterile  
408 razor blade and a single individual *L. squamata* (~190 µm) were added to 4 µl of Qiagen REPLI-  
409 g Advanced Single Cell Storage Buffer using a sterilized Irwin Loop as input for amplification  
410 using the Qiagen REPLI-g Advanced Single Cell kit following the manufacturer's protocol (i.e.,  
411 lysis with SDS and denaturation at room temperature, incubation at 30°C for 2 hours, 60°C for  
412 10 minutes, and 4°C until purification). Resulting amplified DNA, 14.92 µg from *L. squamata*  
413 and 8.74 µg from *C. elegans* were sent to Hudson Alpha Discovery for sequencing on a shared  
414 single PacBio Sequel II flow cell, resulting in ½ a flow cell each.

### 415 Assembly

416 HiFi reads were extracted using the pbbioconda extracthifi package and each set of reads was  
417 assembled with Hifiasm v.0.15.2. A reference guided assembly, using the genome of *C. elegans*

418 Bristol N2 was generated for *C. elegans* using RagTag v.2.1.0 (-scaffold) (Alonge et al. 2022)  
419 with default settings. Genome statistics were generated using QUAST v.5.0 (Gurevich et al.  
420 2013), and completeness was measured with BUSCO 4.0.2 (Simão et al. 2015). [Table 1,2]  
421 Completeness of all assemblies was analyzed with the BUSCO metazoa\_odb10 BUSCO set, and  
422 additionally, both the *de novo* and reference guided *C. elegans* assemblies were assessed with the  
423 nematoda\_odb10 BUSCO set. HiFi reads were mapped back to their respective assemblies using  
424 Minimap2 v.2.22 (Li 2018). The *C. elegans* and *L. squamata* assemblies were searched against  
425 the UniProt reference proteomes database with Diamond 2.0.14 (Buchfink et al. 2015) using the  
426 following settings: diamond blastx --db ~/databases/uniprot\_taxonmap.diamond --query  
427 assembly\_bp.p\_ctg.fasta --outfmt 6 qseqid staxids bitscore qseqid sseqid pident length mismatch  
428 gapopen qstart qend sstart send evalue bitscore --sensitive --max-target-seqs 1 --evalue 1e-25 --  
429 threads 32. The output of these tools as well as BUSCO were used as input for Blobtools.  
430 Further, the *de novo* *C. elegans* assembly was aligned to the publicly available reference *C.*  
431 *elegans* N2 genome (GCA\_000002985.3) to assess completeness and screen for the presence of  
432 chimeric reads as identified by Alvis v.1.0 (Martin and Leggett 2021), a program that identifies  
433 chimeras in the assembly based on mapping statistics from mapping raw reads to the assembled  
434 genome. All *de novo* assemblies (*C. elegans* and *L. squamata*) were screened for contamination  
435 using Blobtools2 v2.6.1 by removing all contigs that had top BLAST hits to taxa other than  
436 Metazoa or “no-hit” when searched against the NCBI non-redundant protein database.

437 Annotation

438 The repeat content of the contaminant filtered *L. squamata* genome was assessed using  
439 RepeatModeler (Flynn et al. 2020) and soft masked using RepeatMasker (Smit et al. 2015). Raw  
440 transcript reads from the publicly available *L. squamata* transcriptome ([SRR1273732](https://doi.org/10.1101/2024.01.17.576123)) were

441 downloaded, quality trimmed with TrimGalore v.0.6.10 from NCBI and mapped against the soft  
442 masked genome using STAR (Dobin et al. 2013). The soft masked genome and mapped  
443 transcripts were given to the BRAKER (Hoff et al. 2019) pipeline as input to produce gene  
444 annotations with the following command: braker.pl --useexisting --cores 12 --softmasking --  
445 UTR=on --crf --makehub --gff3 --species=Lepidodermella\_squamata --genome  
446 Lepidodermella\_sp.asm.bp.p\_ctg\_filtered.fasta.masked --bam RNaseq.bam. Gene annotations  
447 were measured for completeness using the BUSCO metazoa\_odb10 database.

448 Read Coverage Estimation

449 Assemblies of all three data sources (*L. squamata* and amplified and non-amplified *C. elegans*)  
450 were used as subjects to map HiFi reads as a query to estimate genome coverage and coverage  
451 bias. Following read mapping with Minimap2 v.2.22, Bedtools v.2.30.0 (Quinlan 2014) was used  
452 to separate the genomes into independent 100 Kbp windows in which both overall read coverage,  
453 mean coverage, repeat content and GC content were calculated. Resulting graphs were  
454 constructed in the R computing environment (R Core Team 2022). Lorenz graphs were  
455 constructed utilizing the package *gglorenz*. Additionally, we assessed coverage uniformity of our  
456 *C. elegans* HiFi data mapped against the reference genome, as well as PacBio HiFi reads  
457 generated from unamplified DNA extracted for a pool of worms of the same strain  
458 (SRR22507561). Read depth, breadth, and mapping rate for *C. elegans* to the reference assembly  
459 were calculated using SAMtools.

460 Orthology Inference and Supermatrix Construction

461 To investigate the phylogenetic position of Gastrotricha, orthology determination and  
462 supermatrix assembly were performed following a modification of the pipeline of Kocot et al.

463 (2017b) implementing new versions of the programs used if applicable. Lophotrochozoan  
464 genomes (including *L. squamata*) broadly spanning the diversity of the group were selected  
465 along with five outgroup taxa resulting in 28 OTUs. Homologous sequences were identified  
466 using OrthoFinder v.2.4.0 (Emms and Kelly 2019) and sequences shorter than 100 amino acids  
467 were removed, keeping the longest sequence. Homogroups were retained if they included greater  
468 than 75% of the total of all taxa, with those with less being removed. Fasta files were aligned  
469 with MAFFT v.7.310 (Katoh 2002), suspected mistranslated regions removed with HmmCleaner  
470 (Di Franco et al. 2019), and regions high in gaps or ambiguity were trimmed with BMGE  
471 v.1.12.2 (Criscuolo and Gribaldo 2010). Maximum likelihood gene trees were generated using  
472 IQ-Tree 2 (Minh et al. 2020) with the best-fitting model of amino acid substitution for each gene.  
473 Subsequent fasta files and trees were used as input for PhyloPyPruner v.0.9.5  
474 (<https://pypi.org/project/phyloypypruner>) to retrieve a set of strict [1:1] orthologs with the settings  
475 phyloypypruner --min-taxa 15 --min-support 0.9 --mask pdist --trim-lb 3 --trim-divergent 0.75 --  
476 min-pdist 0.01 --prune LS. The --min-taxa flag guaranteed removal of pruned alignments that did  
477 not include at least 15 taxa from the original dataset.

478 Maximum Likelihood Estimation

479 The final supermatrix from PhyloPyPruner of 676,632 amino acid positions was used for  
480 phylogeny reconstruction in IQ-Tree2. Using maximum likelihood with the simplest profile  
481 mixture model available, LG+C20+F, a guide tree for PMSF (Wang et al. 2018) was produced.  
482 The PMSF analysis fitted the C60 profile mixture model, LG+C60+F, to the data and  
483 reconstructed the phylogeny assessing nodal support with 1000 rapid bootstraps.

484

485 **Availability of data and materials**

486 Genomic data generated for this study have been deposited in the NCBI SRA and Genome  
487 databases under the BioProject accession number PRJNA1063365. Scripts used for assembly,  
488 annotation, read coverage investigation, and visualization are available at  
489 [https://github.com/ngroberts/MDA\\_Hifi\\_Roberts\\_2023](https://github.com/ngroberts/MDA_Hifi_Roberts_2023).

490

491 **Competing interests**

492 The authors declare that they have no competing interests.

493

494 **Funding**

495 KMK, NGR, funding from NSF (NSF DEB-1846174) and the University of Alabama the  
496 College Academy of Research, Scholarship, and Creative Activity (CARSCA) grant. THS,  
497 funding from the Research Council of Norway (FRIMEDBIO Project Number 300587).

498

499 **Authors' contributions**

500 Study design, NGR, KMK. Genome assembly, sequencing, and annotation, NGR, KMK, THS.  
501 Statistical analyses and data visualization, NGR, MJG, THS. Manuscript preparation, NGR,  
502 KMK.

503

504 **References:**

505 Alonge M, Lebeigle L, Kirsche M, Jenike K, Ou S, Aganezov S, Wang X, Lippman ZB, Schatz  
506 MC, Soyk S. 2022. Automated assembly scaffolding using RagTag elevates a new  
507 tomato system for high-throughput genome editing. *Genome Biology* 23:258.

508 Thalen, F. *phylopypruner* · PyPI. Available from: <https://pypi.org/project/phylopypruner/>

509 Benita Y, Oosting RS, Lok MC, Wise MJ, Humphery-Smith I. 2003. Regionalized GC content of  
510 template DNA as a predictor of PCR success. *Nucleic Acids Research* 31:e99.

511 Bennett LW. 1979. Experimental Analysis of the Trophic Ecology of *Lepidodermella*  
512 *squammatata* (Gastrotricha: Chaetonotida) in Mixed Culture. *Transactions of the American*  
513 *Microscopical Society* 98:254–260.

514 Birky CW Jr. 1996. Heterozygosity, Heteromorphy, and Phylogenetic Trees in Asexual  
515 Eukaryotes. *Genetics* 144:427–437.

516 Bleidorn C. 2019. Recent progress in reconstructing lophotrochozoan (spiralian) phylogeny. *Org*  
517 *Divers Evol* 19:557–566.

518 Borgström E, Paterlini M, Mold JE, Frisen J, Lundeberg J. 2017. Comparison of whole genome  
519 amplification techniques for human single cell exome sequencing. Li Y, editor. *PLoS*  
520 *ONE* 12:e0171566.

521 de Bourcy CFA, De Vlaminck I, Kanbar JN, Wang J, Gawad C, Quake SR. 2014. A Quantitative  
522 Comparison of Single-Cell Whole Genome Amplification Methods. Wang K, editor.  
523 *PLoS ONE* 9:e105585.

524 Buchfink B, Xie C, Huson DH. 2015. Fast and sensitive protein alignment using DIAMOND.  
525 *Nat Methods* 12:59–60.

526 C. elegans Sequencing Consortium. 1998. Genome sequence of the nematode *C. elegans*: a  
527 platform for investigating biology. *Science* 282:2012–2018.

528 Chapman AR, He Z, Lu S, Yong J, Tan L, Tang F, Xie XS. 2015. Single Cell Transcriptome  
529 Amplification with MALBAC. Lee JW, editor. *PLoS ONE* 10:e0120889.

530 Cohen-Fix O, Askjaer P. 2017. Cell Biology of the *Caenorhabditis elegans* Nucleus. *Genetics*  
531 205:25–59.

532 Criscuolo A, Gribaldo S. 2010. BMGE (Block Mapping and Gathering with Entropy): a new  
533 software for selection of phylogenetic informative regions from multiple sequence  
534 alignments. *BMC Evol Biol* 10:210.

535 Cunha TJ, de Medeiros BAS, Lord A, Sørensen MV, Giribet G. 2023. Rampant loss of universal  
536 metazoan genes revealed by a chromosome-level genome assembly of the parasitic  
537 Nematomorpha. *Current Biology* 33:3514-3521.e4.

538 Dean FB, Hosono S, Fang L, Wu X, Faruqi AF, Bray-Ward P, Sun Z, Zong Q, Du Y, Du J, et al.  
539 2002. Comprehensive human genome amplification using multiple displacement  
540 amplification. *Proc. Natl. Acad. Sci. U.S.A.* 99:5261–5266.

541 Dean FB, Nelson JR, Giesler TL, Lasken RS. 2001. Rapid Amplification of Plasmid and Phage  
542 DNA Using Phi29 DNA Polymerase and Multiply-Primed Rolling Circle Amplification.  
543 *Genome Res.* 11:1095–1099.

544 Di Franco A, Poujol R, Baurain D, Philippe H. 2019. Evaluating the usefulness of alignment  
545 filtering methods to reduce the impact of errors on evolutionary inferences. *BMC Evol  
546 Biol* 19:21.

547 Dobin A, Davis CA, Schlesinger F, Drenkow J, Zaleski C, Jha S, Batut P, Chaisson M, Gingeras  
548 TR. 2013. STAR: ultrafast universal RNA-seq aligner. *Bioinformatics* 29:15–21.

549 Dujardin F. 1841. Histoire naturelle des zoophytes: Infusoires, comprenant la physiologie et la  
550 classification de ces animaux, et la manière de les étudier à l'aide du microscope:  
551 Ouvrage accompagné de planches. Roret

552 Edgecombe GD, Giribet G, Dunn CW, Hejnol A, Kristensen RM, Neves RC, Rouse GW,  
553 Worsaae K, Sørensen MV. 2011. Higher-level metazoan relationships: recent progress  
554 and remaining questions. *Org Divers Evol* 11:151–172.

555 Emms DM, Kelly S. 2019b. OrthoFinder: phylogenetic orthology inference for comparative  
556 genomics. *Genome Biol* 20:238.

557 Evrony GD, Lee E, Mehta BK, Benjamini Y, Johnson RM, Cai X, Yang L, Haseley P, Lehmann  
558 HS, Park PJ, et al. 2015. Cell Lineage Analysis in Human Brain Using Endogenous  
559 Retroelements. *Neuron* 85:49–59.

560 Flot J-F, Hespeels B, Li X, Noel B, Arkhipova I, Danchin EGJ, Hejnol A, Henrissat B, Koszul R,  
561 Aury J-M, et al. 2013. Genomic evidence for ameiotic evolution in the bdelloid rotifer  
562 *Adineta vaga*. *Nature* 500:453–457.

563 Flynn JM, Hubley R, Goubert C, Rosen J, Clark AG, Feschotte C, Smit AF. 2020.  
564 RepeatModeler2 for automated genomic discovery of transposable element families.  
565 *Proceedings of the National Academy of Sciences* 117:9451–9457.

566 Fontaneto D, Kieneke A, Kristensen R, Maas A, Riemann O, Rothe B, Sørensen M, Sterrer W,  
567 Taraschewski H, Warner L. 2015. Gastrotricha and Gnathifera.

568 Fu Y, Li C, Lu S, Zhou W, Tang F, Xie XS, Huang Y. 2015. Uniform and accurate single-cell  
569 sequencing based on emulsion whole-genome amplification. *Proc Natl Acad Sci USA*  
570 112:11923–11928.

571 Garmendia C, Bernad A, Esteban JA, Blanco L, Salas M. 1992. The bacteriophage phi 29 DNA  
572 polymerase, a proofreading enzyme. *Journal of Biological Chemistry* 267:2594–2599.

573 Gurevich A, Saveliev V, Vyahhi N, Tesler G. 2013. QUAST: quality assessment tool for genome  
574 assemblies. *Bioinformatics* 29:1072–1075.

575 Hejnol A. 2015. Gastrotricha. In: Wanninger A, editor. Evolutionary Developmental Biology of  
576 Invertebrates 2: Lophotrochozoa (Spiralia). Vienna: Springer. p. 13–19. Available from:  
577 [https://doi.org/10.1007/978-3-7091-1871-9\\_2](https://doi.org/10.1007/978-3-7091-1871-9_2)

578 Hoff K, Lomsadze A, Borodovsky M, Stanke M. 2019. Whole-Genome Annotation with  
579 BRAKER. *Methods Mol Biol* 1962:65–95.

580 Hon T, Mars K, Young G, Tsai Y-C, Karalius JW, Landolin JM, Maurer N, Kudrna D, Hardigan  
581 MA, Steiner CC, et al. 2020. Highly accurate long-read HiFi sequencing data for five  
582 complex genomes. *Sci Data* 7:399.

583 Hosono S, Faruqi AF, Dean FB, Du Y, Sun Z, Wu X, Du J, Kingsmore SF, Egholm M, Lasken  
584 RS. 2003. Unbiased Whole-Genome Amplification Directly From Clinical Samples.  
585 *Genome Res.* 13:954–964.

586 Huang S, Kang M, Xu A. 2017. HaploMerger2: rebuilding both haploid sub-assemblies from  
587 high-heterozygosity diploid genome assembly. Berger B, editor. *Bioinformatics* 33:2577–  
588 2579.

589 Katoh K. 2002. MAFFT: a novel method for rapid multiple sequence alignment based on fast  
590 Fourier transform. *Nucleic Acids Research* 30:3059–3066.

591 Kocot KM. 2016. On 20 years of Lophotrochozoa. *Org Divers Evol* 16:329–343.

592 Kocot KM, Struck TH, Merkel J, Waits DS, Todt C, Brannock PM, Weese DA, Cannon JT,  
593 Moroz LL, Lieb B, et al. 2017. Phylogenomics of Lophotrochozoa with Consideration of  
594 Systematic Error. *Systematic Biology* 66:256–282.

595 Laetsch DR, Blaxter ML. 2017. BlobTools: Interrogation of genome assemblies. *F1000Res*  
596 6:1287.

597 Lasken RS. 2007. Single-cell genomic sequencing using Multiple Displacement Amplification.  
598 *Current Opinion in Microbiology* 10:510–516.

599 Lasken RS, Egholm M. 2003. Whole genome amplification: abundant supplies of DNA from  
600 precious samples or clinical specimens. *Trends in Biotechnology* 21:531–535.

601 Lasken RS, Stockwell TB. 2007. Mechanism of chimera formation during the Multiple  
602 Displacement Amplification reaction. *BMC Biotechnol* 7:19.

603 Laumer CE. 2018. Inferring Ancient Relationships with Genomic Data: A Commentary on  
604 Current Practices. *Integrative and Comparative Biology* 58:623–639.

605 Laumer, C. Picogram input multimodal sequencing (PiMmS) v1.  
606 <https://doi.org/10.17504/protocols.io.rm7vzywy5lx1/v1> (2022).

607 Laumer CE, Bekkouche N, Kerbl A, Goetz F, Neves RC, Sørensen MV, Kristensen RM, Hejnol  
608 A, Dunn CW, Giribet G, et al. 2015. Spiralian Phylogeny Informs the Evolution of  
609 Microscopic Lineages. *Current Biology* 25:2000–2006.

610 Laumer CE, Fernández R, Lemer S, Combosch D, Kocot KM, Riesgo A, Andrade SCS, Sterrer  
611 W, Sørensen MV, Giribet G. 2019. Revisiting metazoan phylogeny with genomic  
612 sampling of all phyla. *Proc. R. Soc. B.* 286:20190831.

613 Lee Y-C, Ke H-M, Liu Y-C, Lee H-H, Wang M-C, Tseng Y-C, Kikuchi T, Tsai IJ. 2023. Single-  
614 worm long-read sequencing reveals genome diversity in free-living nematodes. *Nucleic  
615 Acids Research* 51:8035–8047.

616 Li H. 2018. Minimap2: pairwise alignment for nucleotide sequences. Birol I, editor.  
617 *Bioinformatics* 34:3094–3100.

618 Li J, Lu N, Tao Y, Duan M, Qiao Y, Xu Y, Ge Q, Bi C, Fu J, Tu J, et al. 2018. Accurate and  
619 sensitive single-cell-level detection of copy number variations by micro-channel multiple  
620 displacement amplification (μcMDA). *Nanoscale* 10:17933–17941.

621 Manni M, Berkeley MR, Seppey M, Simão FA, Zdobnov EM. 2021. BUSCO Update: Novel and  
622 Streamlined Workflows along with Broader and Deeper Phylogenetic Coverage for  
623 Scoring of Eukaryotic, Prokaryotic, and Viral Genomes. *Molecular Biology and  
624 Evolution* 38:4647–4654.

625 Margulis L, Schwartz KV. 1998. Five Kingdoms: an illustrated guide to the Phyla of life on  
626 earth. 3rd edition. Available from:  
627 <https://www.marinespecies.org/aphia.php?p=sourcedetails&id=3>

628 Marlétaz F, Peijnenburg KTCA, Goto T, Satoh N, Rokhsar DS. 2019. A New Spiralian  
629 Phylogeny Places the Enigmatic Arrow Worms among Gnathiferans. *Current Biology*  
630 29:312-318.e3.

631 Martin S, Leggett RM. 2021. Alvis: a tool for contig and read ALignment VISualisation and  
632 chimera detection. *BMC Bioinformatics* 22:124.

633 Martín-Durán JM, Vellutini BC, Marlétaz F, Cetrangolo V, Cveticic N, Thiel D, Henriet S,  
634 Grau-Bové X, Carrillo-Baltodano AM, Gu W, et al. 2021. Conservative route to genome  
635 compaction in a miniature annelid. *Nat Ecol Evol* 5:231–242.

636 Mikhailov KV, Slyusarev GS, Nikitin MA, Logacheva MD, Penin AA, Aleoshin VV, Panchin  
637 YV. 2016. The Genome of *Intosha linei* Affirms Orthonectids as Highly Simplified  
638 Spiralianians. *Curr Biol* 26:1768–1774.

639 Minh BQ, Schmidt HA, Chernomor O, Schrempf D, Woodhams MD, von Haeseler A, Lanfear  
640 R. 2020. IQ-TREE 2: New Models and Efficient Methods for Phylogenetic Inference in  
641 the Genomic Era. *Molecular Biology and Evolution* 37:1530–1534.

642 Nelson JR. 2014. Random-Primed, Phi29 DNA Polymerase-Based Whole Genome  
643 Amplification. *Current Protocols in Molecular Biology* [Internet] 105. Available from:  
644 <https://onlinelibrary.wiley.com/doi/10.1002/0471142727.mb1513s105>

645 Pinard R, de Winter A, Sarkis GJ, Gerstein MB, Tartaro KR, Plant RN, Egholm M, Rothberg  
646 JM, Leamon JH. 2006. Assessment of whole genome amplification-induced bias through  
647 high-throughput, massively parallel whole genome sequencing. *BMC Genomics* 7:216.

648 Pollard MO, Gurdasani D, Mentzer AJ, Porter T, Sandhu MS. 2018. Long reads: their purpose  
649 and place. *Human Molecular Genetics* 27:R234–R241.

650 Quinlan AR. 2014. BEDTools: The Swiss-Army Tool for Genome Feature Analysis. *Current  
651 Protocols in Bioinformatics* 47:11.12.1-11.12.34.

652 R Core Team. 2022. R: A Language and Environment for Statistical Computing. Vienna,  
653 Austria: R Foundation for Statistical Computing Available from: <https://www.R-project.org/>

655 Rayko M, Komissarov A, Kwan JC, Lim-Fong G, Rhodes AC, Kliver S, Kuchur P, O'Brien SJ,  
656 Lopez JV. 2020. Draft genome of *Bugula neritina*, a colonial animal packing powerful  
657 symbionts and potential medicines. *Sci Data* 7:356.

658 Rodrigue S, Malmstrom RR, Berlin AM, Birren BW, Henn MR, Chisholm SW. 2009. Whole  
659 Genome Amplification and De novo Assembly of Single Bacterial Cells. *PLOS ONE*  
660 4:e6864.

661 Sahdev S, Saini S, Tiwari P, Saxena S, Singh Saini K. 2007. Amplification of GC-rich genes by  
662 following a combination strategy of primer design, enhancers and modified PCR cycle  
663 conditions. *Molecular and Cellular Probes* 21:303–307.

664 Schneider C, Woehle C, Greve C, D'Haese CA, Wolf M, Hiller M, Janke A, Bálint M, Huettel  
665 B. 2021. Two high-quality *de novo* genomes from single ethanol-preserved specimens of  
666 tiny metazoans (Collembola). *GigaScience* 10:giab035.

667 Seo H-C, Kube M, Edvardsen RB, Jensen MF, Beck A, Spriet E, Gorsky G, Thompson EM,  
668 Lehrach H, Reinhardt R, et al. 2001. Miniature Genome in the Marine Chordate  
669 *Oikopleura dioica*. *Science* 294:2506–2506.

670 Simão FA, Waterhouse RM, Ioannidis P, Kriventseva EV, Zdobnov EM. 2015. BUSCO:  
671 assessing genome assembly and annotation completeness with single-copy orthologs.  
672 *Bioinformatics* 31:3210–3212.

673 Simion P, Belkhir K, François C, Veyssier J, Rink JC, Manuel M, Philippe H, Telford MJ. 2018.  
674 A software tool ‘CroCo’ detects pervasive cross-species contamination in next generation  
675 sequencing data. *BMC Biol* 16:28.

676 Smit A, Hubley R, Green P. 2015. RepeatMasker Open-4.0. 2013–2015.

677 Stevens L, Martínez-Ugalde I, King E, Wagah M, Absolon D, Bancroft R, Gonzalez de la Rosa  
678 P, Hall JL, Kieninger M, Kloch A, et al. 2023. Ancient diversity in host-parasite  
679 interaction genes in a model parasitic nematode. *Nat Commun* 14:7776.

680 Struck TH, Wey-Fabrizius AR, Golombek A, Hering L, Weigert A, Bleidorn C, Klebow S,  
681 Iakovenko N, Hausdorf B, Petersen M, et al. 2014. Platyzoan Paraphyly Based on  
682 Phylogenomic Data Supports a Noncoelomate Ancestry of Spiralia. *Molecular Biology  
and Evolution* 31:1833–1849.

684 Telenius H, Carter NP, Bebb CE, Nordenskjöld M, Ponder BAJ, Tunnacliffe A. 1992.  
685 Degenerate oligonucleotide-primed PCR: General amplification of target DNA by a  
686 single degenerate primer. *Genomics* 13:718–725.

687 Wang H-C, Minh BQ, Susko E, Roger AJ. 2018. Modeling Site Heterogeneity with Posterior  
688 Mean Site Frequency Profiles Accelerates Accurate Phylogenomic Estimation.  
689 *Systematic Biology* 67:216–235.

690 Worsaae K, Vinther J, Sørensen MV. 2023. Evolution of Bilateria from a Meiofauna  
691 Perspective—Miniaturization in the Focus. In: New Horizons in Meiobenthos Research.  
692 Springer, Cham. p. 1–31. Available from: [https://link.springer.com/chapter/10.1007/978-3-031-21622-0\\_1](https://link.springer.com/chapter/10.1007/978-3-031-21622-0_1)

694 Zhou W, Emery SB, Flasch DA, Wang Y, Kwan KY, Kidd JM, Moran JV, Mills RE. 2020.  
695 Identification and characterization of occult human-specific LINE-1 insertions using  
696 long-read sequencing technology. *Nucleic Acids Research* 48:1146–1163.

697 Zong C, Lu S, Chapman AR, Xie XS. 2012. Genome-Wide Detection of Single Nucleotide and  
698 Copy Number Variations of a Single Human Cell. *Science* 338:1622–1626.

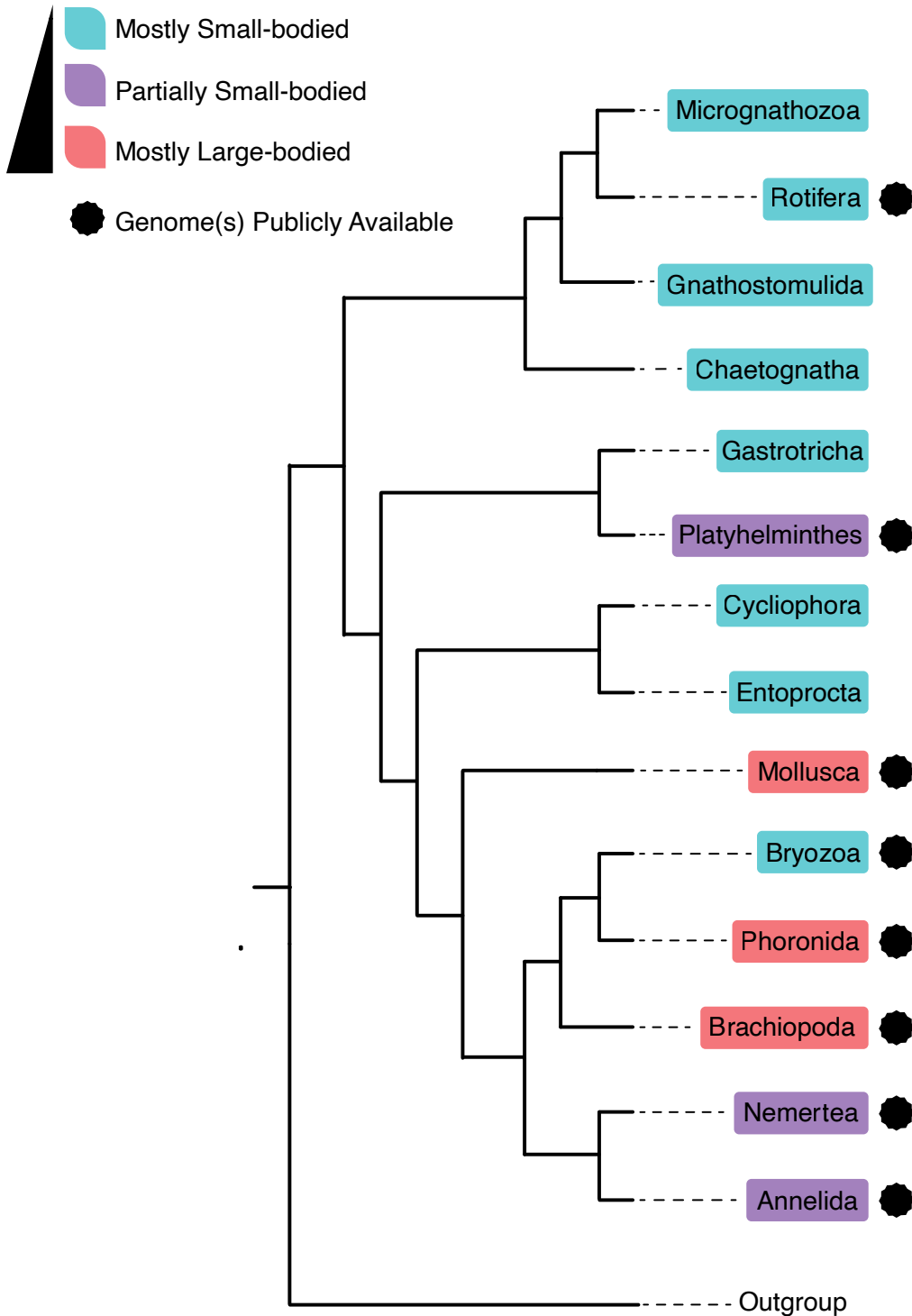
699

700

701

702

703



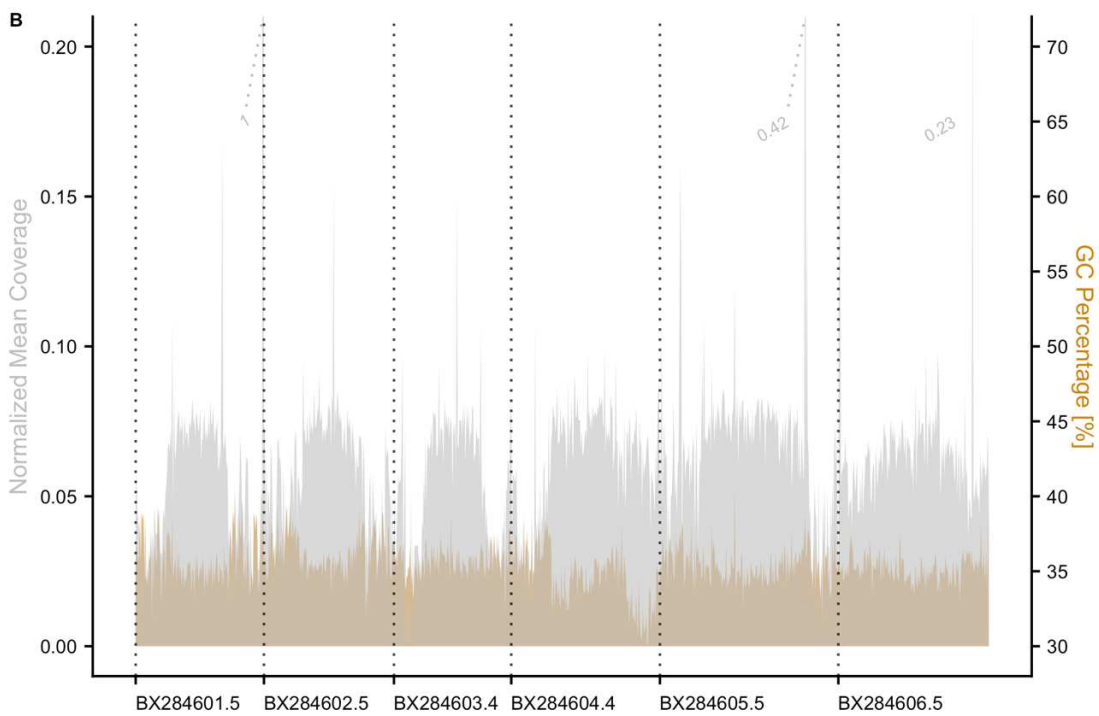
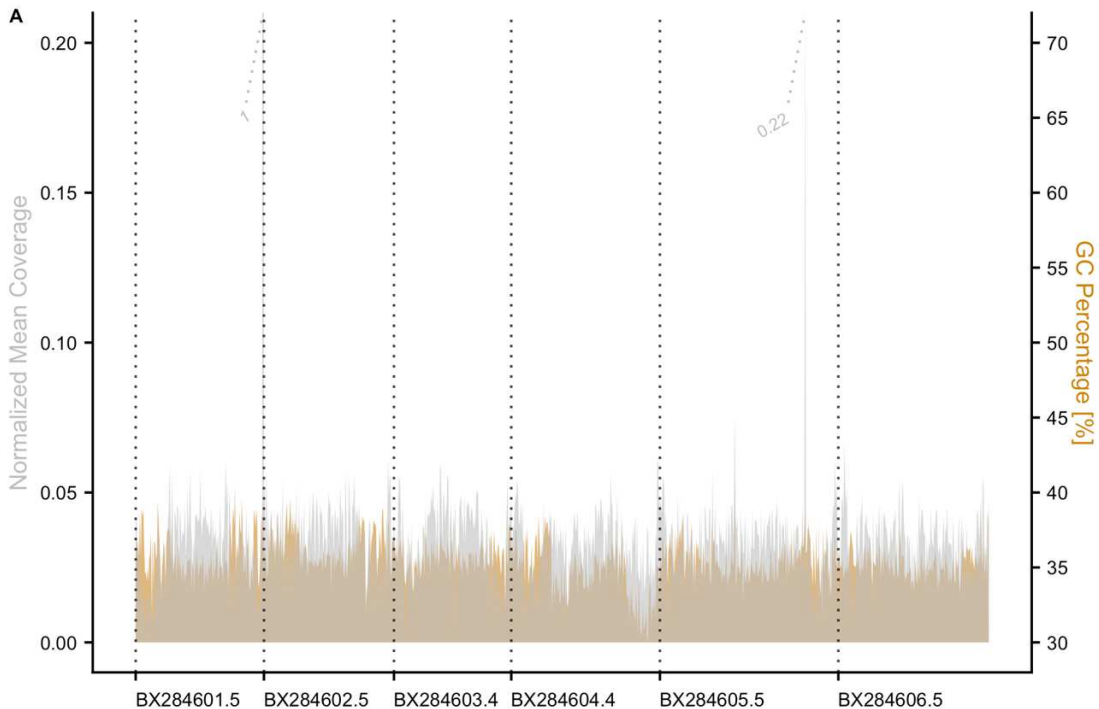
704

705 **Figure 1.** Phyla within Lophotrochozoa that are exclusively, partially, or mostly small-bodied.

706 Those with one or more publicly available genomes are indicated. Tree modified from Laumer et

707 al. (2019).

*Caenorhabditis elegans*



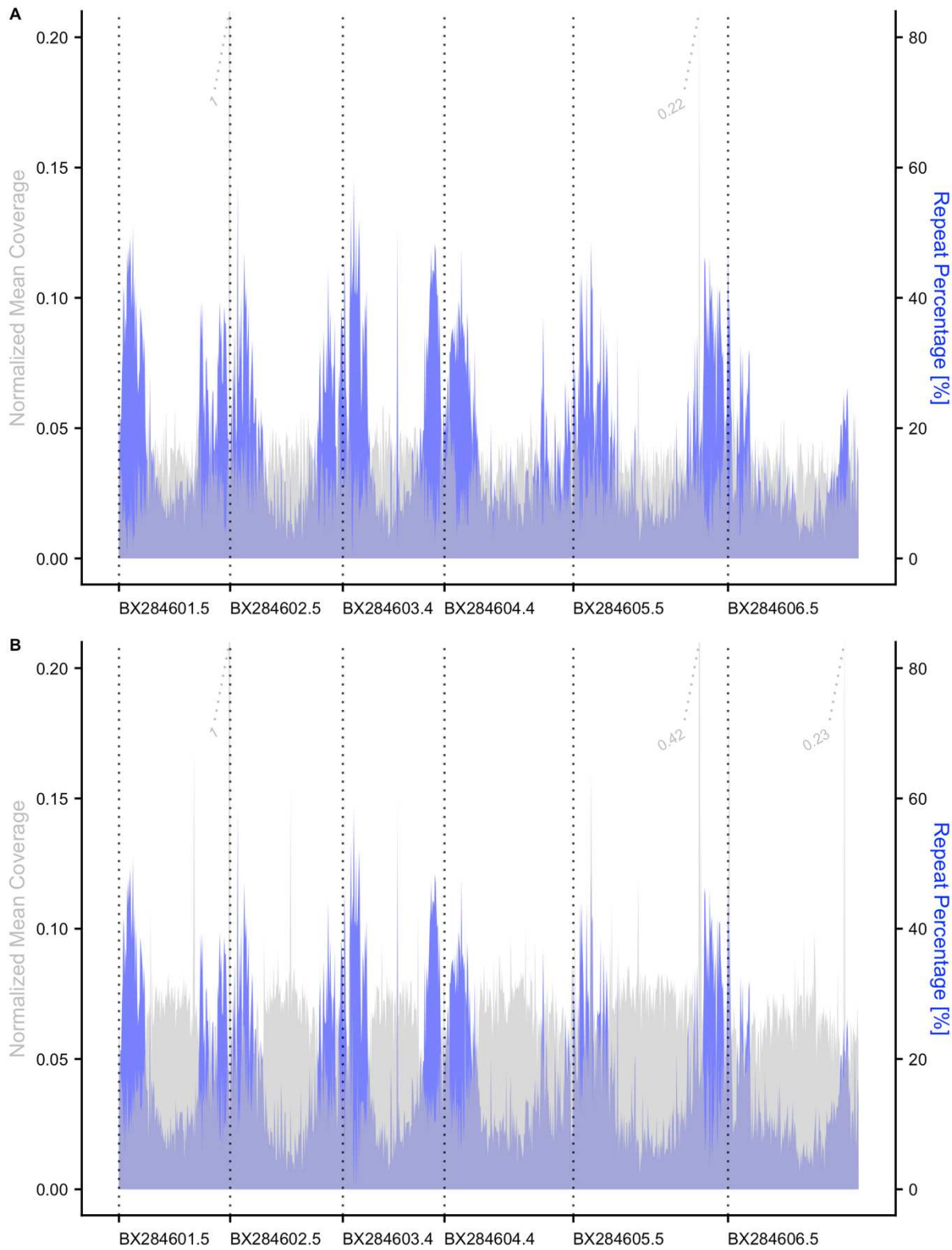
708

709

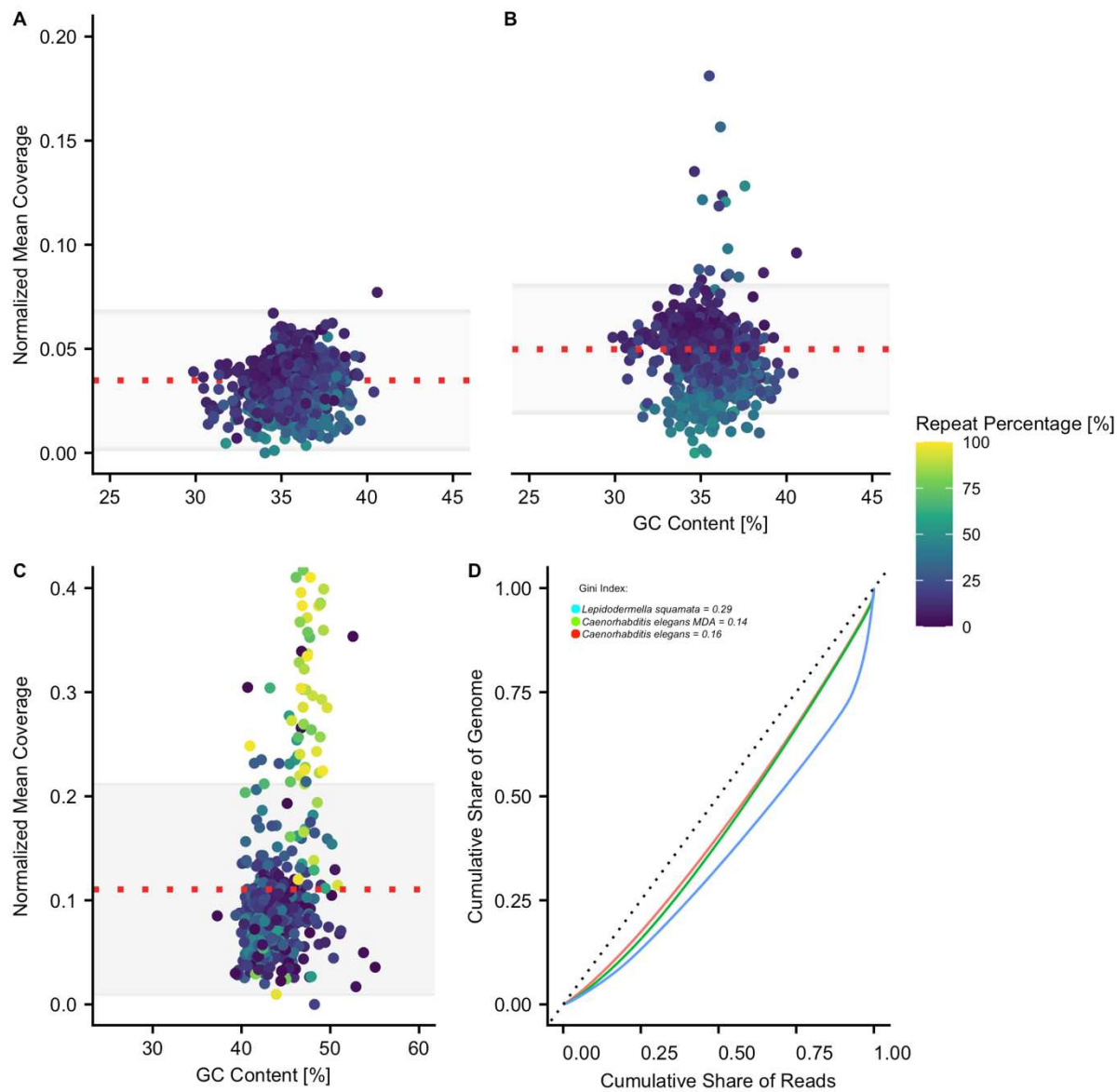
710

711 **Figure 2.** Mean coverage and GC content across 100 Kbp blocks of the *C. elegans* reference  
712 genome. A. Coverage of PacBio HiFi reads from MDA DNA aligned to the reference *C. elegans*  
713 genome [Gray] alongside GC percentage [Orange]. B. Coverage of unamplified PacBio HiFi  
714 reads aligned to the reference *C. elegans* genome [Gray] alongside GC percentage [Orange].

*Caenorhabditis elegans*



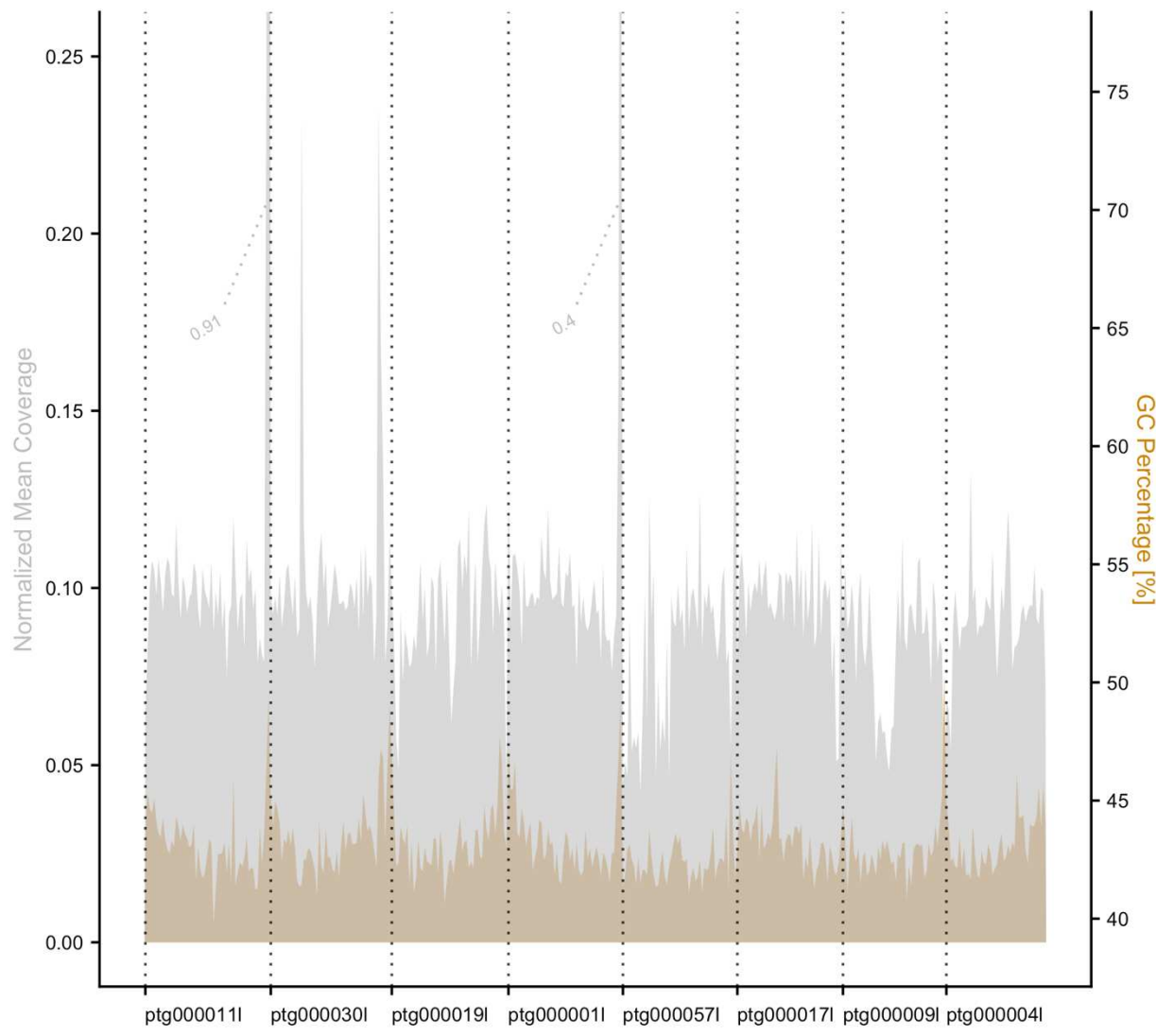
716 **Figure 3.** Mean coverage and repeat content across 100 Kbp blocks of the *C. elegans* reference  
717 genome. A. Coverage of PacBio HiFi reads from MDA DNA aligned to the reference *C. elegans*  
718 genome [Gray] alongside repeat content [Blue]. B. Coverage PacBio HiFi reads from  
719 unamplified DNA from a pool of worms aligned to the reference genome [Gray] alongside repeat  
720 content [Blue].



721

722

723 **Figure 4.** Normalized coverage, GC content, and repeat percentage of each genome assembly in  
724 100 Kbp blocks. A. Dotplot showing coverage of MDA amplified reads with respect to GC  
725 content for 100 Kbp blocks of the *C. elegans* reference genome. B. Dotplot showing coverage of  
726 non-amplified reads from a pool of worms with respect to GC content for 100 Kbp blocks of the  
727 *C. elegans* reference genome. C. Dotplot showing coverage with respect to GC content for  
728 contigs in the *L. squamata* genome assembly based on MDA DNA. A-C. Repeat content of each  
729 contig is indicated according to the key at the top right of the figure. D. Lorenz curves and Gini  
730 values for each assembly indicating coverage uniformity. The diagonal line represents perfect  
731 read coverage uniformity.



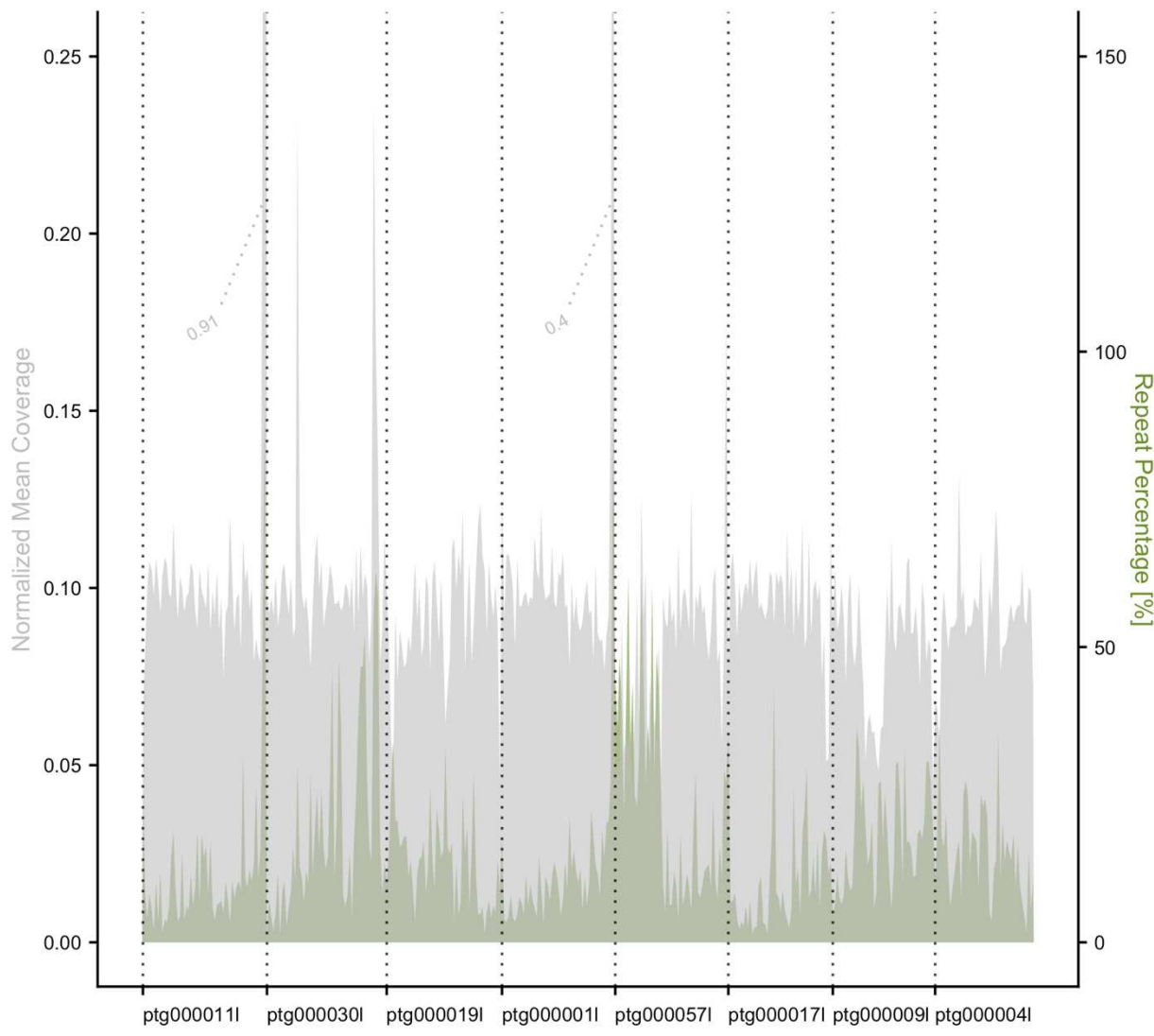
732

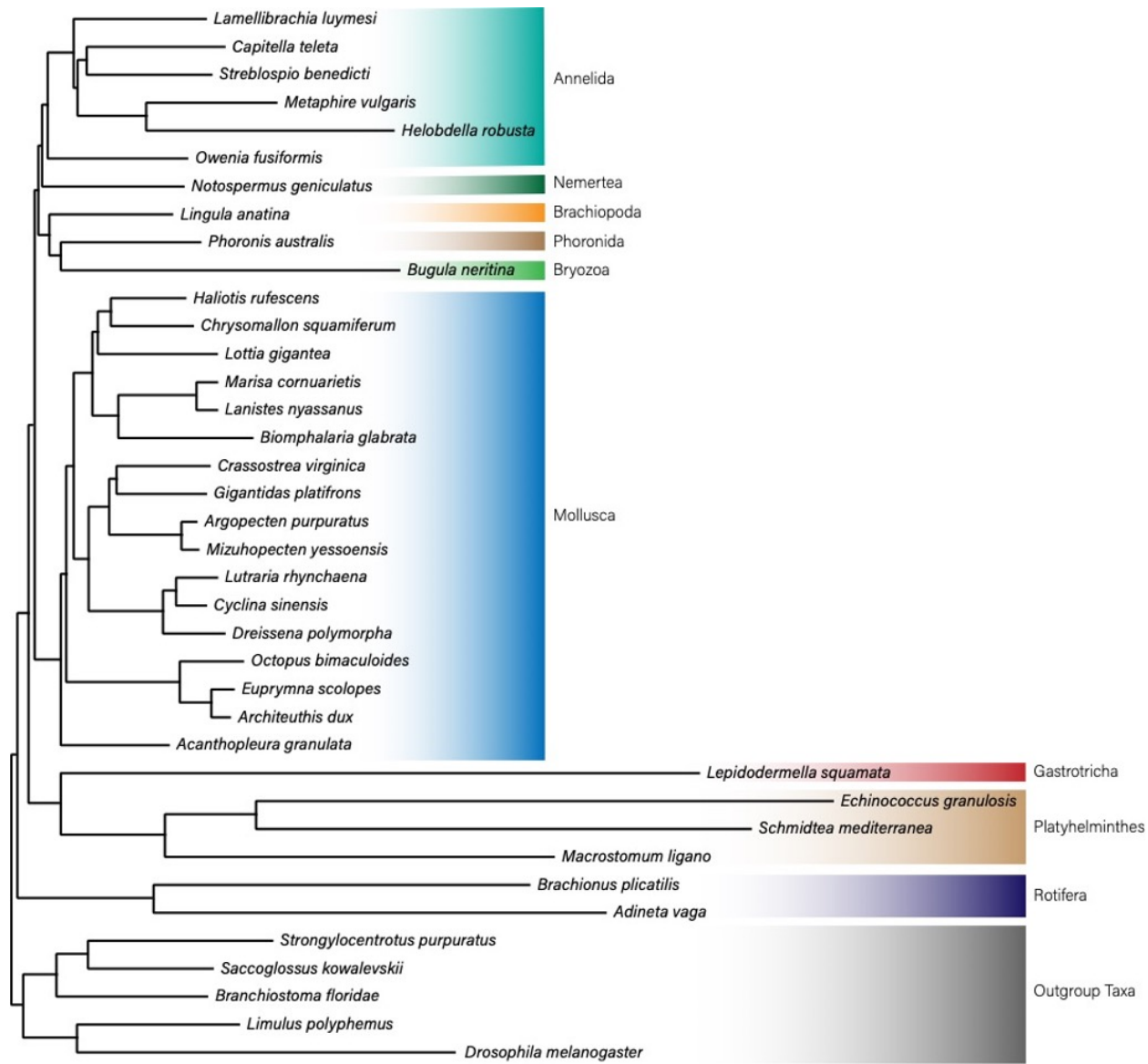
733 **Figure 5.** Coverage and GC content across 100 Kbp blocks of the eight largest contigs of the *L.*  
734 *squamata* genome. Coverage of PacBio HiFi reads from MDA DNA aligned to the 8 largest  
735 contigs of the *de novo* *L. squamata* genome assembly [Gray] alongside GC percentage [Orange].

736

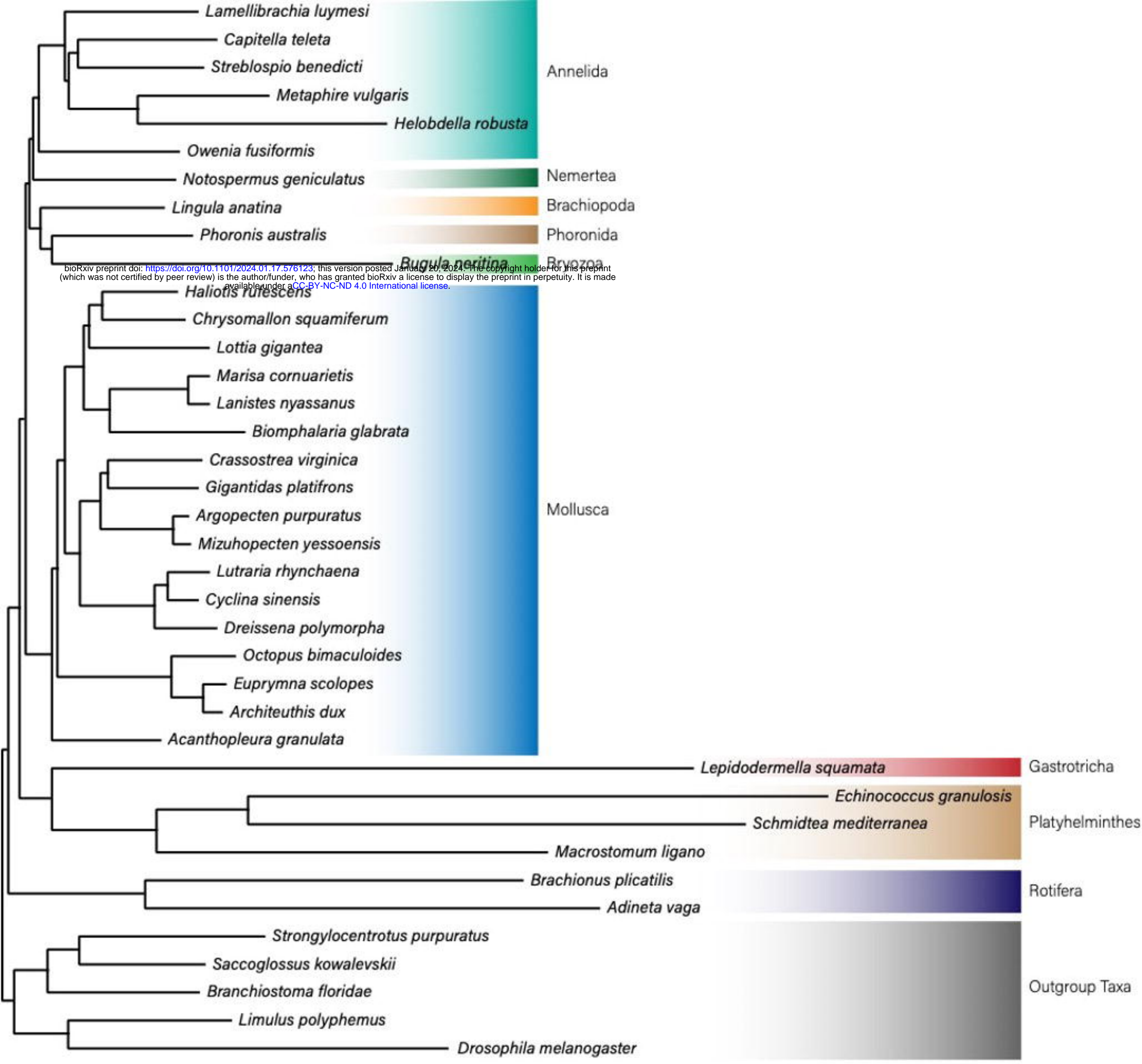
737

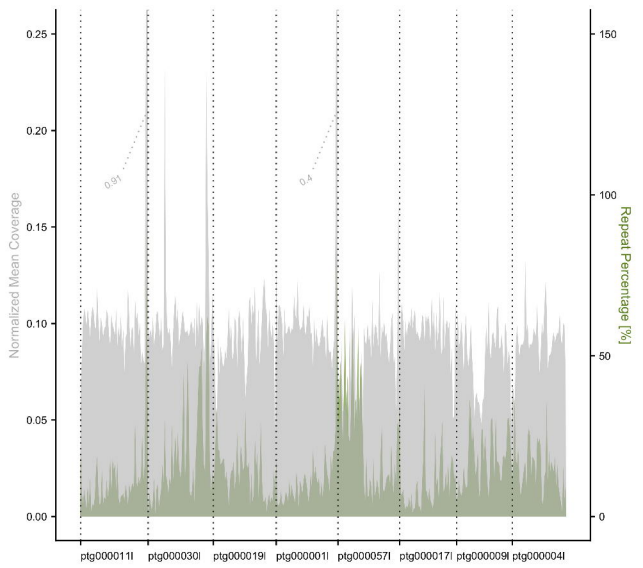
738

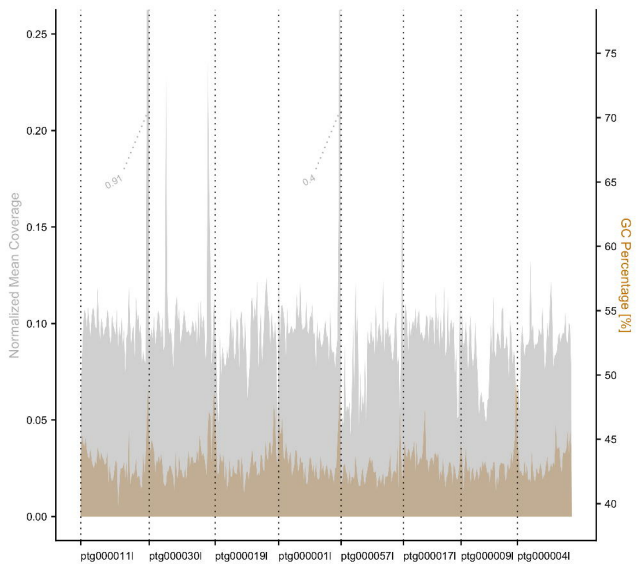


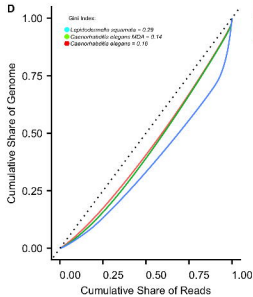
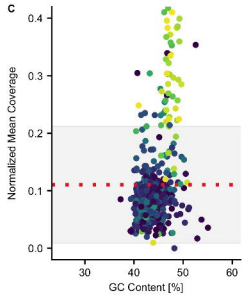
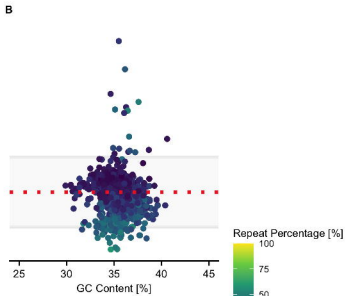
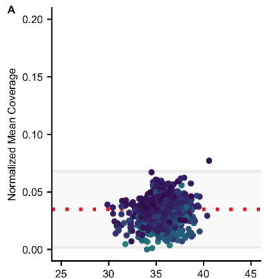


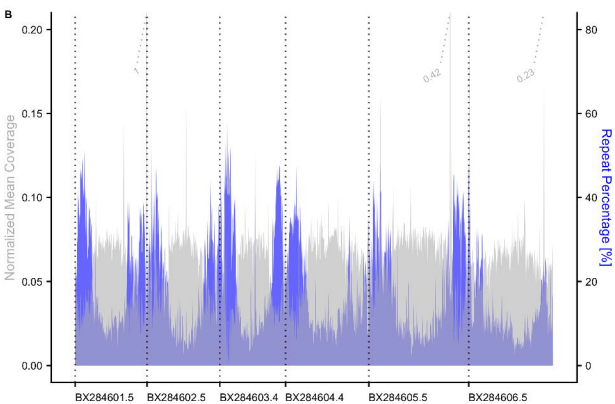
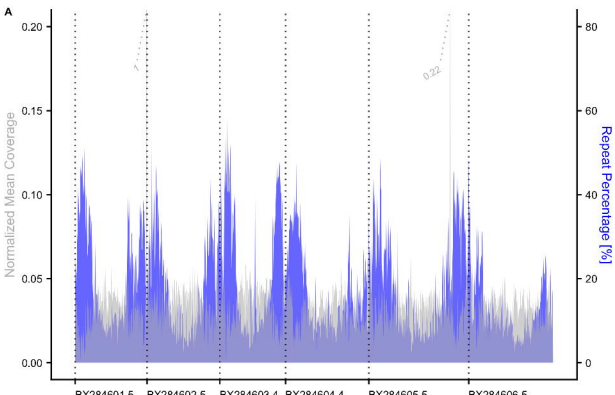
748 **Figure 7.** Evolutionary relationships of lophotrochozoan taxa with genomic data sequenced to  
749 date placing Gastrotricha as the sister taxon of Platyhelminthes (Rouphozoa). IQ-TREE 2  
750 analysis of 676,632 amino acid positions with 18.68% missing data using the PMSF  
751 (LG+C60+F) with LG+C20+F as the guide tree. All nodes have 100% bootstrap support.

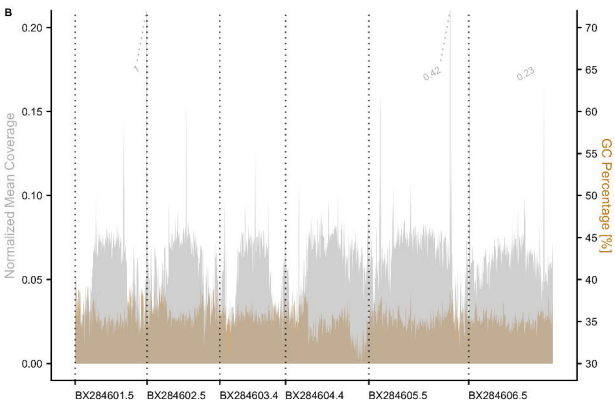
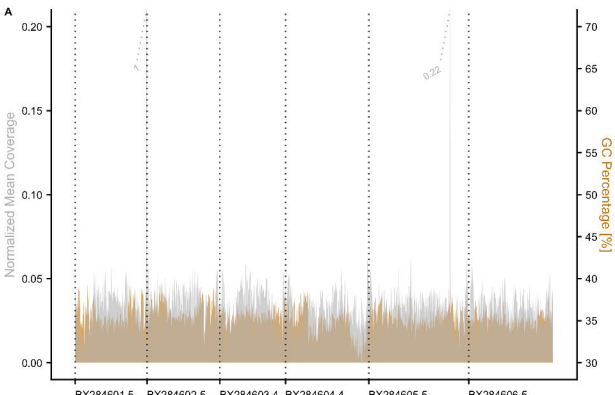














Mostly Small-bodied



Partially Small-bodied



Mostly Large-bodied



Genome(s) Publicly Available

